AD 745117

6

.....contributing to man's
understanding of the environment world

EVALUATION OF THE LASA, ALPA, NORSAR LONG PERIOD NETWORK

H. MACK
SEISMIC ARRAY ANALYSIS CENTER

17 APRIL 1972

Prepared for
AIR FORCE TECHNICAL APPLICATIONS CENTER
Washington, D.C.

Under
Project VELA UNIFORM

Sponsored by
ADVANCED RESEARCH PROJECTS AGENCY
Nuclear Monitoring Research Office
ARPA Order No.1620

DDC
RECEIVED
JUN 28 1972
C

Reproduced by
NATIONAL TECHNICAL
INFORMATION SERVICE
U S Department of Commerce
Springfield VA 22151

TELEDYNE GEOTECH
ALEXANDRIA LABORATORIES

APPROVED FOR PUBLIC RELEASE; DISTRIBUTION UNLIMITED.

62

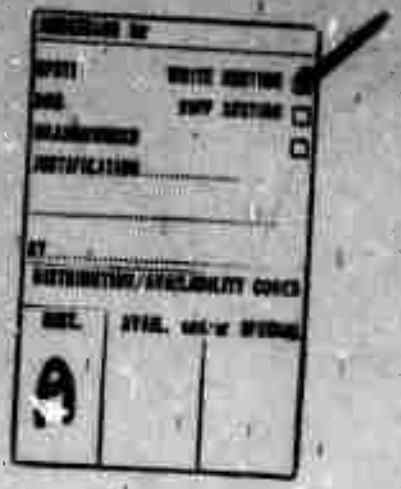

Neither the Advanced Research Projects Agency nor the Air Force Technical Applications Center will be responsible for information contained herein which has been supplied by other organizations or contractors, and this document is subject to later revision as may be necessary. The views and conclusions presented are those of the authors and should not be interpreted as necessarily representing the official policies, either expressed or implied, of the Advanced Research Projects Agency, the Air Force Technical Applications Center, or the U S Government.

Unclassified
Security Classification

DOCUMENT CONTROL DATA - R&D
(Security classification of title, body of abstract and indexing annotation must be entered when the overall report is classified)

1. ORIGINATING ACTIVITY (Corporate author)
Teledyne Geotech
Alexandria, Virginia

2a. REPORT SECURITY CLASSIFICATION
Unclassified

2b GROUP

3 REPORT TITLE
EVALUATION OF THE LASA, ALPA, NORSAR LONG PERIOD NETWORK

4. DESCRIPTIVE NOTES (Type of report and inclusive dates)
Scientific

5. AUTHOR(S) (Last name, first name, initial)
Mack, H.

6. REPORT DATE
17 April 1972

7a. TOTAL NO. OF PAGES
60

7b. NO. OF REFS
6

8a. CONTRACT OR GRANT NO.
F33657-71-C-0510

b. PROJECT NO.
VELA T/1709

c.
ARPA Order No. 1620

d. ARPA Program Code No. 1F10

9a. ORIGINATOR'S REPORT NUMBER(S)
6

9b. OTHER REPORT NO(S) (Any other numbers that may be assigned this report)

10. AVAILABILITY/LIMITATION NOTICES
APPROVED FOR PUBLIC RELEASE; DISTRIBUTION UNLIMITED.

11. SUPPLEMENTARY NOTES

12. SPONSORING MILITARY ACTIVITY
Advanced Research Projects Agency
Nuclear Monitoring Research Office
Washington, D.C.

13 ABSTRACT

This report is an expansion of SAAC Report No. 4. The SAAC long period processing methods, based on frequency-wavenumber analysis, are capable of analyzing all the events reported in the LASA and NORSAR Daily Event Summaries within real-time. The capability of LASA to detect Rayleigh waves is azimuth dependent. A comparison of NORSAR and LASA on a data set of Kurile Islands events resulted in a detection of surface waves from all events with $m_b \geq 4.0$ as reported by the LASA Daily Event Summary. A study of central Asia-western Soviet Union events shows that NORSAR M_S values are consistently higher than those at ALPA or LASA, the lowest level detections being made were on events with $M_S = 2.5$ and 2.7 for the western Soviet Union and central Asia respectively.

14 KEY WORDS
LASA
ALPA
NORSAR
LP NETWORK

I

Unclassified
Security Classification

EVALUATION OF THE LASA, ALPA, NORSAR LONG PERIOD NETWORK SEISMIC ARRAY ANALYSIS CENTER REPORT NO. 6

by H. Mack

AFTAC Project Number:	VELA T/1709
Project Title:	Seismic Array Analysis Center
ARPA Order No.:	1620
ARPA Program Code No.:	1F10
Name of Contractor:	TELEDYNE GEOTECH
Contract No.:	F33657-71-C-0510
Effective Date of Contract:	1 December 1970
Amount of Contract:	$1,034,946
Contract Expiration Date:	31 December 1971
Project Manager:	Wm. C. Dean (703) 836-7647

P. O. Box 334, Alexandria, Virginia

APPROVED FOR PUBLIC RELEASE; DISTRIBUTION UNLIMITED.

II

This research was supported by the Advanced Research Projects Agency, Nuclear Monitoring Research Office, under Project VELA-UNIFORM, and accomplished under the technical direction of the Air Force Technical Applications Center under Contract F33657-71-C-0510.

Neither the advanced Research Projects Agency nor the Air Force Technical Applications Center will be responsible for information contained herein which has been supplied by other organizations or contractors, and this document is subject to later revision as may be necessary. The views and conclusions presented are those of the authors and should not be interpreted as necessarily representing the official policies, either expressed or implied, of the Advanced Research Projects Agency, the Air Force Technical Applications Center, or the U S Government.

ABSTRACT

This report is an expansion of SAAC Report No. 4. The SAAC long period processing methods, based on frequency-wavenumber analysis, are capable of analyzing all the events reported in the LASA and NORSAR Daily Event Summaries within real-time. The capability of LASA to detect Rayleigh waves is azimuth dependent. A comparison of NORSAR and LASA on a data set of Kurile Islands events resulted in a detection of surface waves from all events with $m_b \geq 4.0$ as reported by the LASA Daily Event Summary. A study of central Asia-western Soviet Union events shows that NORSAR M_s values are consistently higher than those at ALPA or LASA, the lowest level detections being made were on events with $M_s = 2.5$ and 2.7 for the western Soviet Union and central Asia respectively.

TABLE OF CONTENTS

LIST OF ILLUSTRATIONS

I. INTRODUCTION

This report describes the long period processing methods developed and applied in the SAAC. Using these methods, a preliminary evaluation is given of the capability of the three large LP arrays, LASA, NORSAR and ALPA, to detect and measure the amplitude of Rayleigh waves associated with P-wave detections reported in the LASA and NORSAR Daily Event Summaries. The phrase "preliminary evaluation" is deliberately used because long period data are now routinely analyzed from all three arrays and so the data on which our evaluation is based are continually increasing. Also our processing methods are continuously revised and improved with a resulting improvement in the capability to detect small signals and separate interfering waves. Thus the results and conclusions presented in this report must be regarded as a current evaluation which will probably be modified as more detection results become available.

II. LP DATA PROCESSING

The choice of data processing methods was influenced by the fact that a large number of events have to be processed in real time. Time-domain beamforming and plotting is a slow process which suffers the disadvantage that the propagation azimuth and velocity must be assumed. Any disturbance visible on a particular beam may be associated with adjacent beams or a side lobe. For these and other reasons, a frequency-wavenumber (f-k) approach has been developed for routine analysis of the LP data. A description of the f-k analysis method, as used in the SAAC, is given in Appendix I. A complete description of the f-k processing system is currently being written as SAAC Report No. 9.

A flow diagram of the process is shown in Figure 1. All the LP data from NORSAR, ALPA and LASA are recorded simultaneously on the SAAC low-rate tape, each tape containing approximately 12 hours of recorded data for each array. The data are used directly from the low-rate tape; no intermediate or event tape is used. A particular time window is selected, based on the P-wave arrival time at LASA. The individual channels are deglitched and edited with noisy and dead channels discarded automatically. The signal-to-noise ratio detection threshold can be set at any level and the velocity range of interest can also be set arbitrarily.

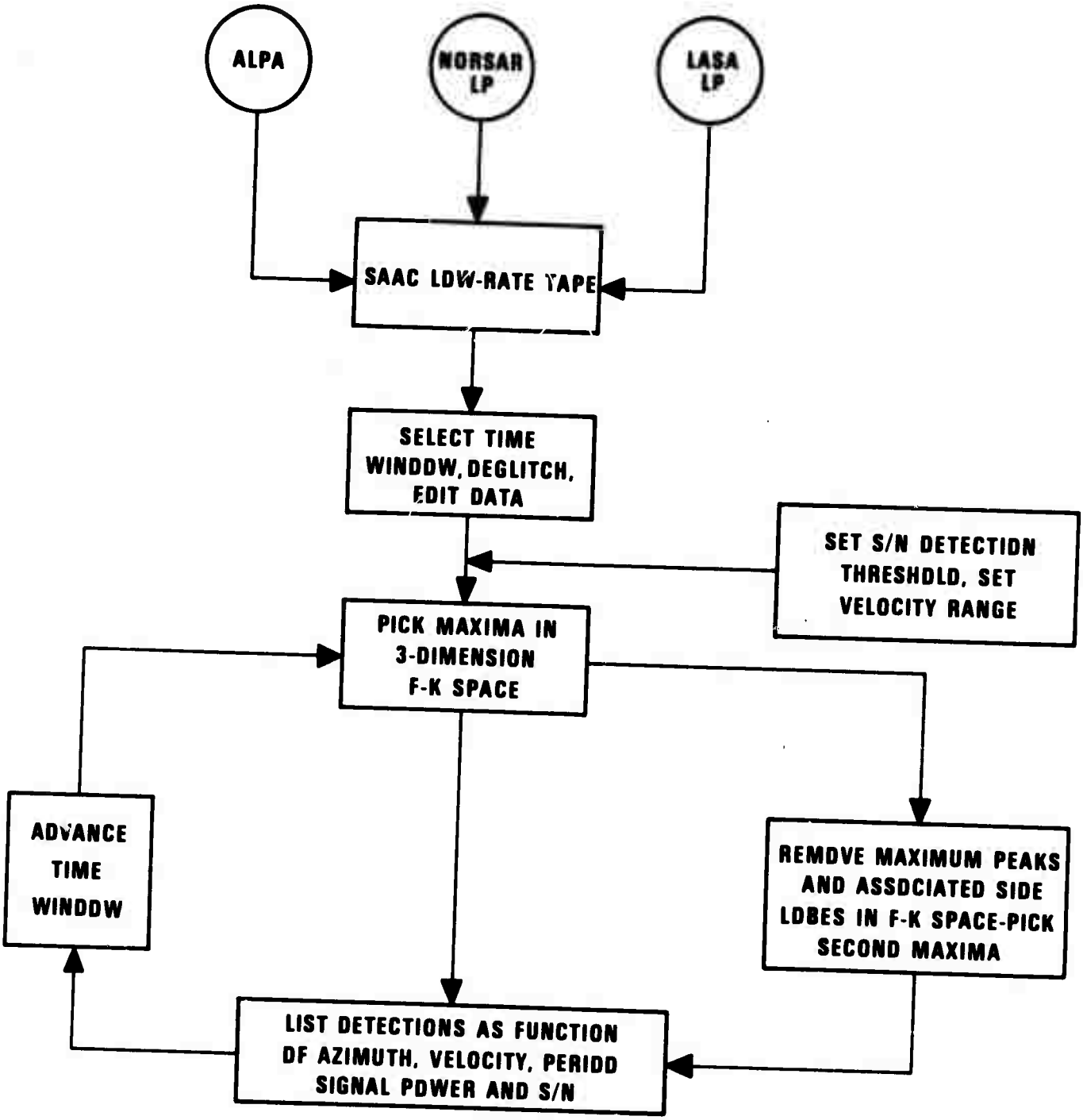

Figure 1. Schematic illustration of the SAAC LP processing program.

The multichannel data are then Fourier transformed. Maxima of power in three-dimensional f-k space are automatically picked, and if they exceed the detection threshold and are in the specified velocity range, these maxima are listed with the corresponding azimuth, velocity, period, signal power estimate and signal-to-noise ratio estimate. An option is then available to detect smaller signals, in which the maximum power peaks and associated side lobes are removed and second maxima are picked. If any of these second maxima satisfy the detection criteria they are also listed as functions of azimuth, etc. The time window is then moved forward or backward in time by any specified amount and the whole process, including the editing, is repeated.

The decision whether a peak corresponds to the expected Rayleigh wave is based on several criteria. First, and most importantly, the time must be correct. Using a 256-second window and 25% overlap, a time resolution of approximately two minutes is obtained for a particular period. This resolution enables the dispersion to be observed and this itself is a basis for decision. Second, the azimuth and phase velocity must be correct. Both of these quantities are dependent on period so the expected values for a particular region and a particular array are obtained by observing large amplitude signals. For low signal-to-noise ratios the

noise can displace the location of a peak in f-k space slightly and hence affect the velocity and azimuth value listed. For such cases, deviations from the expected azimuth of up to 15^{o} are tolerated. Also, the analyzed data are examined for time intervals immediately before and after the detected arrival to see whether the peak is persistent or spasmodic. If spasmodic, the peak is discarded as noise.

The surface wave magnitude M_s is derived from the estimate of the signal power. The details of how this is actually done are described in Appendix II. Time-domain beamforming and plotting programs are available for visual display of the recorded data.

Programs are also available to measure the spatial coherency of signals within the area of an array. The spatial coherency gives a quantitative measure of signal degeneracy at any given frequency and is also diagnostic of the mechanism causing the degeneracy (Mack and Flinn, 1972). A detailed study of the spatial coherence of Rayleigh waves at the three large arrays is currently being written and will appear as SAAC Report No. 8.

III. CONTINUOUS ANALYSIS OF LASA LP DATA

In SAAC Report No. 4, an experiment was described in which 50 days of LASA LP recordings were analyzed. The recording period was in the summer months of July and August. The results are detailed in that previous report but for the sake of completeness the main conclusions will be outlined here. The study showed that the capability of LASA to detect Rayleigh waves, using events listed in the Daily Event Summary, is azimuth dependent. LASA is relatively insensitive to events in South America compared with events to the northwest. This is a function of the respective travel paths and is not caused by azimuthally dependent noise.

The background noise has a major coherent component. This appears as discrete trains of Rayleigh waves propagating across the array from all directions. Because of the relatively short window used in the analysis, the coherent noise does not appear isotropic. Rather a particular window will detect one or two of the discrete wave trains and then, as the window is moved in time, detections will be made from other directions. The 50 days of analysis showed that LASA receives a good deal of coherent noise from azimuths around 60° to 70°. A good deal of energy lies in the microseismic band within the period range of 16 to 18 seconds. However, some appear with periods of around 20 seconds. Hence the

threshold of detections for Rayleigh waves is quite dependent upon the nature and direction of coherent noise at any particular instant. The microseisms from the above mentioned azimuths are considered to be associated with sea wave activity. Triangulation using the other arrays usually puts the main source in the Labrador Sea.

Another important outcome from this study was the effect of a large earthquake on the detection capability of the array. An earthquake near Honshu with $m_b = 6.8$ produced such large surface waves that no further detections were made for approximately four hours. After the initial Rayleigh wave had passed, scattered waves were detected from a variety of azimuths and, even though much smaller than the main arrival, they were sufficiently large to mask Rayleigh waves from smaller earthquakes. Presumably NORSAR and ALPA were similarly affected.

IV. NETWORK EVALUATION

Kuriles Study

SAAC Report No. 4 gave some results of a LASA-NORSAR comparison using events in the Kurile Islands region, an area which is equidistant from the two arrays. This study is continuing and the current state of the evaluation is presented in this report. Now that ALPA is working consistently, events from the Kuriles recorded at ALPA are also being routinely processed and these results are included. A listing of all the events used is given in Appendix III. This listing also gives the result of processing each event for each array.

M_s:m_b plots for the Kuriles events are shown in Figure 2 for LASA and Figure 3 for NORSAR. The two distributions are very similar except for the fact that the NORSAR M_s values are generally higher than those measured at LASA. The difference in travel paths could account for this. Rayleigh waves received at LASA travel through the north Pacific and the Aleutian arc, then through western Canada, altogether a rather complex path. The path from the Kuriles to NORSAR may be considered a bit simpler as the bulk of the propagation occurs through the northern part of the Asian continent. Marshall and Basham (1972) suggest a correction of +0.13 to an M_s value measured on a wave propagating over a mixed path relative to the M_s value measured on a wave

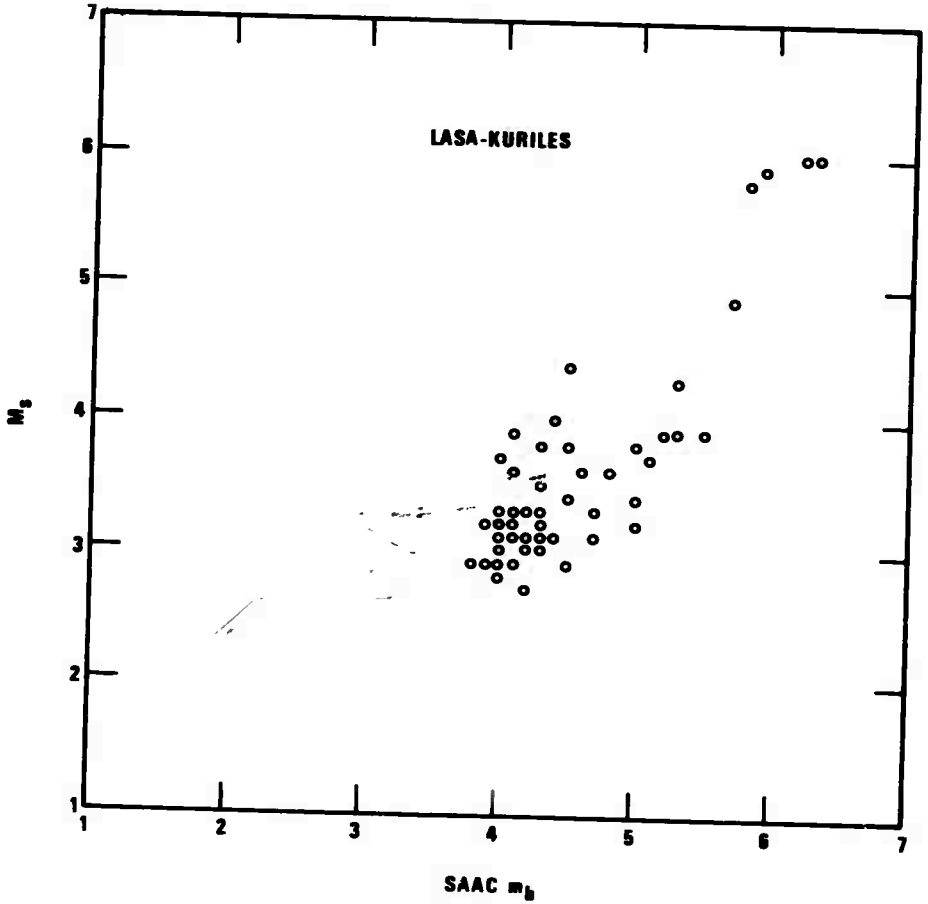

Figure 2. LASA M_s:m_b measurements for a set of events from the Kurile Islands region.

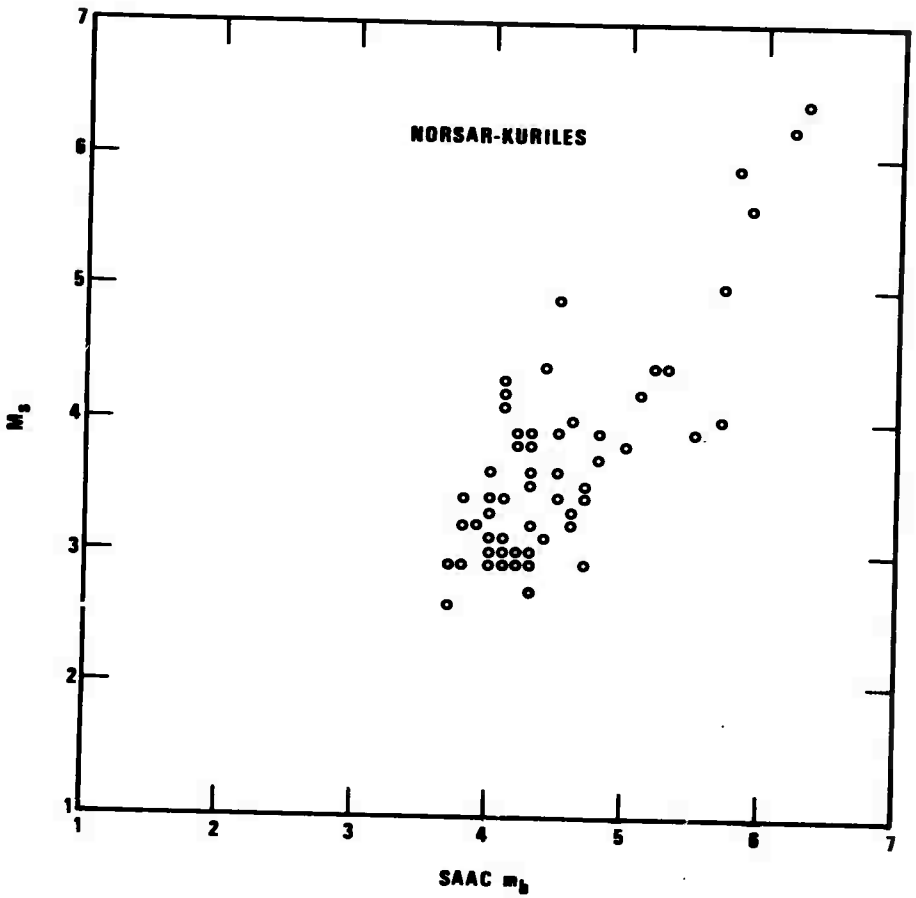

Figure 3. NORSAR M_s:m_b measurements for a set of events from the Kurile Islands region.

traveling in a continental structure only. This suggestion generally agrees with the data presented in this report.

It is of interest to note that each of these two M_s : m_b distributions may possibly indicate the two distinct groups suggested by Lacoss (1971).

Figures 4 and 5 show a breakdown of the Kurile Islands events in terms of detection and non-detection. All events reported by the SAAC in the period May - December 1971 for which $4.0 \leq m_b \leq 5.0$ have been used. The hatched areas denote events missed due to the presence of another larger surface wave in the time period when a Rayleigh wave from the area of interest was expected. These interfering waves arrived on azimuths close to the back azimuth from the Kurile Islands and so array processing, even the "stripping" mentioned in the data processing section, was not of any help. In the magnitude range $4.5 \leq m_b \leq 4.9$ the three events missed at each array because of interference were the same. In the range $4.0 \leq m_b \leq 4.4$ the four missed at NORSAR were also hidden by interference at LASA. The fifth event hidden at LASA was detected at NORSAR. Very few events were missed when there was no apparent interference. For body wave magnitudes greater than or equal to 4.0, as reported in the SAAC Daily Event Summary, only one was not detected at NORSAR. This had $m_b = 4.1$ and it was, in fact, detected at LASA. Of the three not

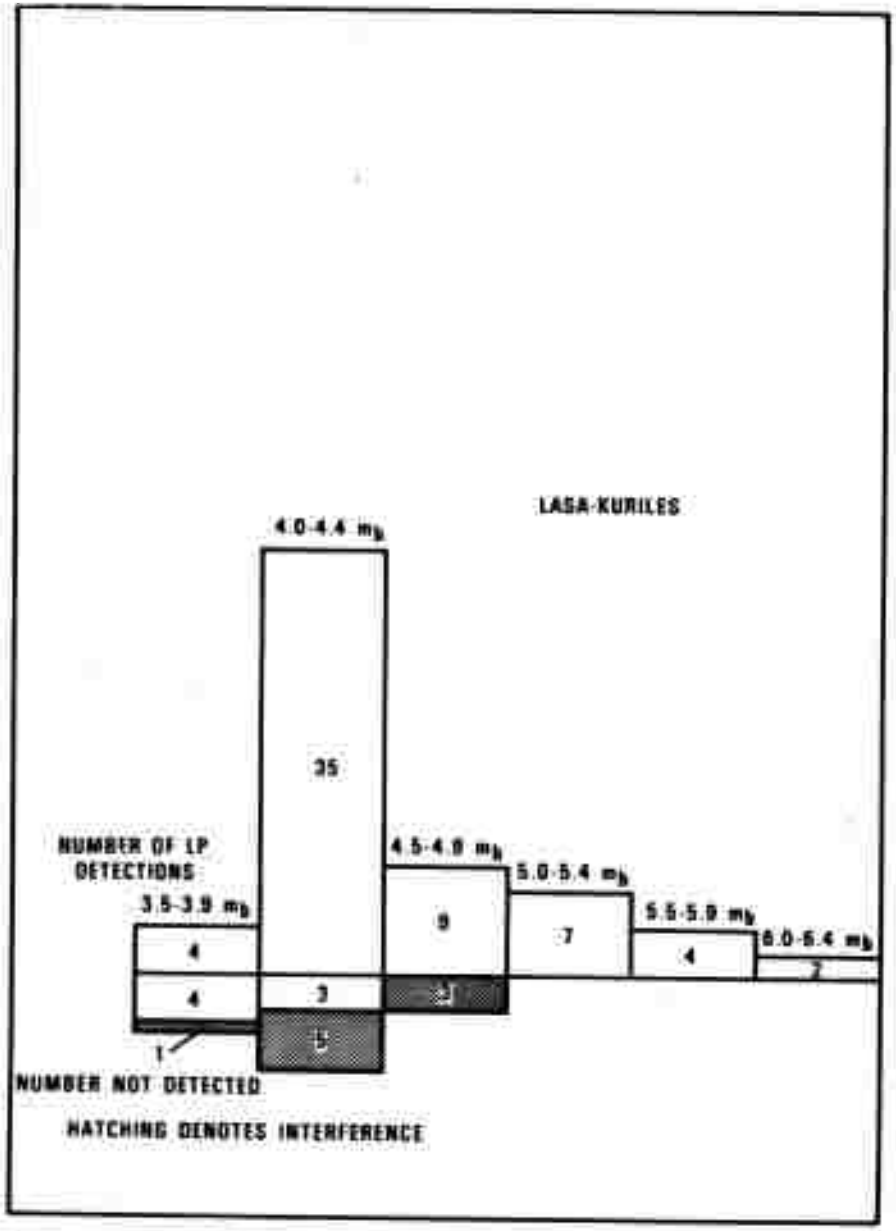

Figure 4. Number of LP detections/non-detections versus SAAC m_b for the Kurile Islands region event set recorded at LASA.

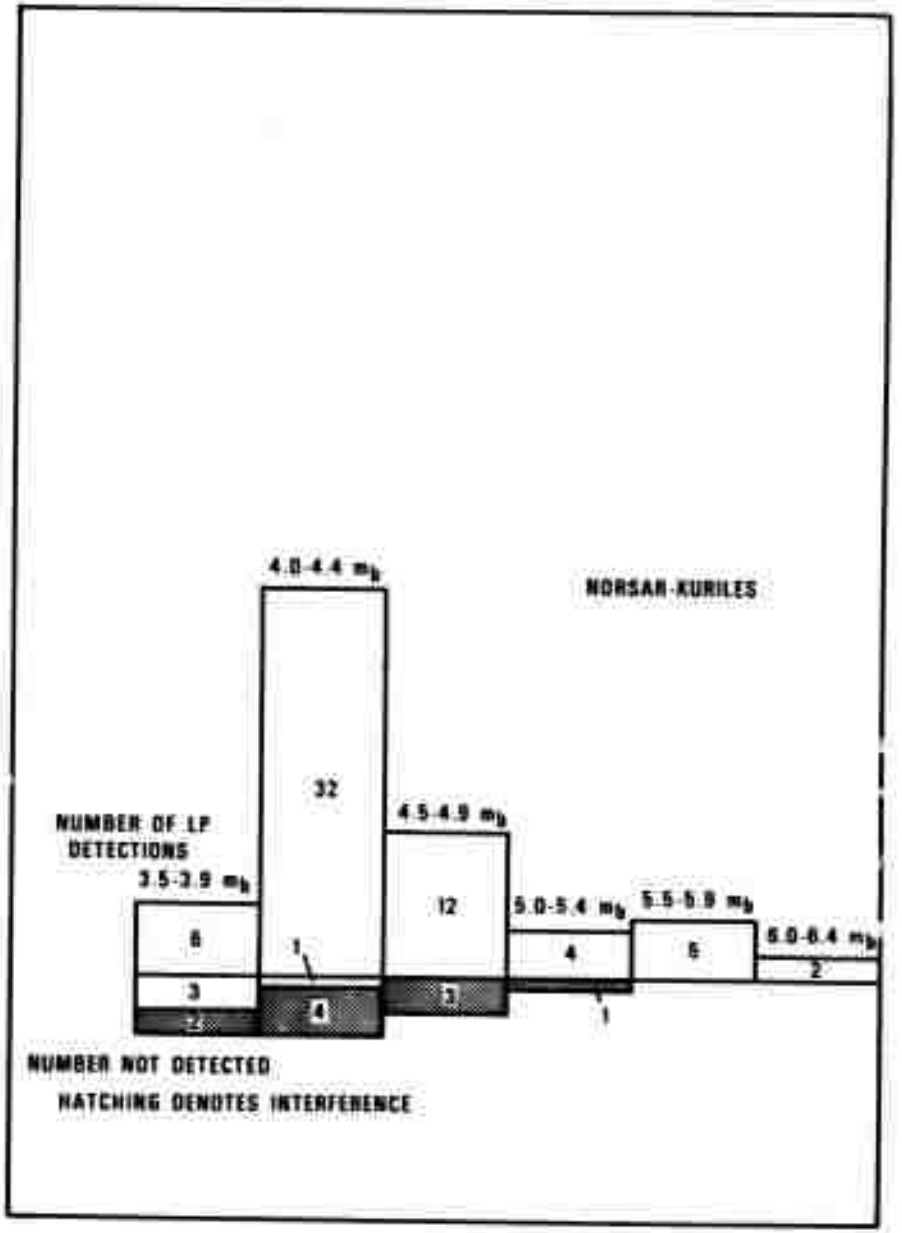

Figure 5. Number of LP detections/non-detections versus SAAC m_b for the Kurile Islands region event set recorded at NORSAR.

detected at LASA two were detected at NORSAR and for the other, the NORSAR data were bad on the low-rate tape. If we accept that a detection at just one of the two arrays is, in fact, a true detection then apart from one miss at LASA when the NORSAR data were bad, all events with $m_b \geq 4.0$, as reported by the SAAC Daily Event Summary, were detected when there was no obvious interference. It would appear, therefore that for SAAC $m_b \sim 4.0$ the most serious cause of non-detection of events in the Kurile Islands is interference from other events. Approximately 15% of this data set could not be detected at either array due to interference.

Processing of events with SAAC $m_b \leq 4.0$ is currently being done in order to try to establish some working threshold for the Kurile Islands region.

Central Asia-western Soviet Union

ALPA and NORSAR are conveniently situated for studying surface waves emanating from the Sino-Soviet region. The ray paths from a particular event to each array are approximately orthogonal but are generally not equidistant except for a region covering Lake Baikal, eastern Mongolia and the eastern part of China. However, as the central Asian-western Soviet Union region is of particular interest, an ALPA-NORSAR comparison has been made using events from that area rather than from a more localized source region such as the Kuriles in the LASA-NORSAR study.

The data from ALPA has been generally good only since October 1971. The NORSAR data, transmitted via the TAL, has improved towards the end of that year also. The study has, therefore, been essentially confined to events occurring fairly recently. Another, and more serious qualification on this evaluation is that much of the region in question is at or beyond the teleseismic limit of P-wave detection for LASA. Thus LASA has a relatively high threshold of detection for events in that area and the body wave magnitude measurements can differ quite drastically from those reported by NOAA. The NORSAR Daily Summary is not edited in a similar manner to the LASA Daily Event Summary, so we have to refer to the NORSAR bulletin which is the NORSAR EP output trans-

mitted via the TAL; this has been available only recently. Presumably this bulletin has the same shortcomings as the SAAC EP output bulletin (SAAC Report No. 1) and hence must be used with caution. However, for events in the central Asian region the body wave magnitudes reported by NORSAR tend to be more in agreement with the NOAA values and so, wherever possible, these values are taken in preference to the LASA-SAAC values.

The list of events used is tabulated in Appendix III together with the M_s values at each array if available. More measurements were obtained from NORSAR because the data were consistently better. Currently this situation has improved and good data are being received from both arrays at comparable rates.

Although these events are by no means a complete data set, no particular selection rules have been applied and so the results are most probably representative of a larger set. Only events reported by NOAA as being deep (> 60 km) have been omitted. Some deep events may be included. Very few small magnitude events ($m_b \leq 4.0$) are included simply because they do not pass the LASA-SAAC EP threshold. This situation is being remedied as we become more familiar with the NORSAR bulletin.

Figure 6 shows M_s:m_b values for NORSAR. Good separation between earthquakes and presumed explosions is observed. Figure 7 gives the equivalent values for

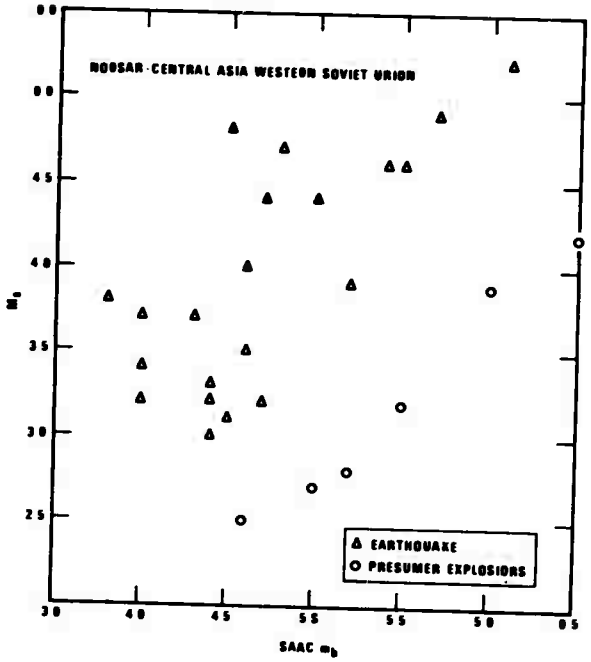

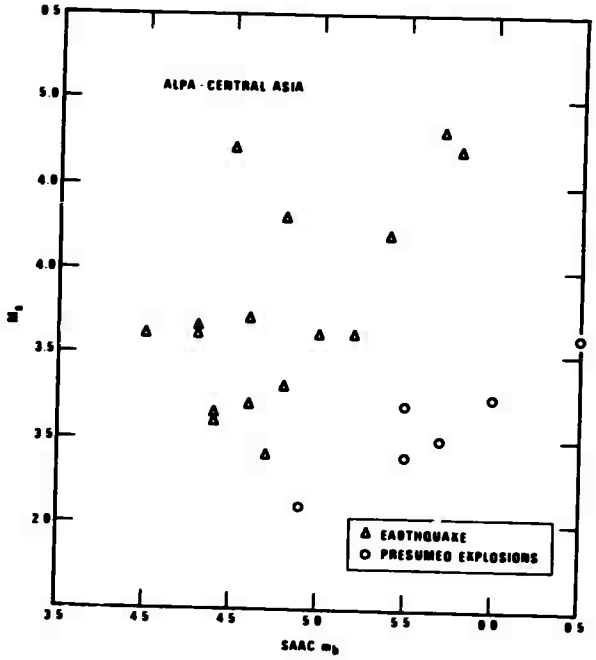

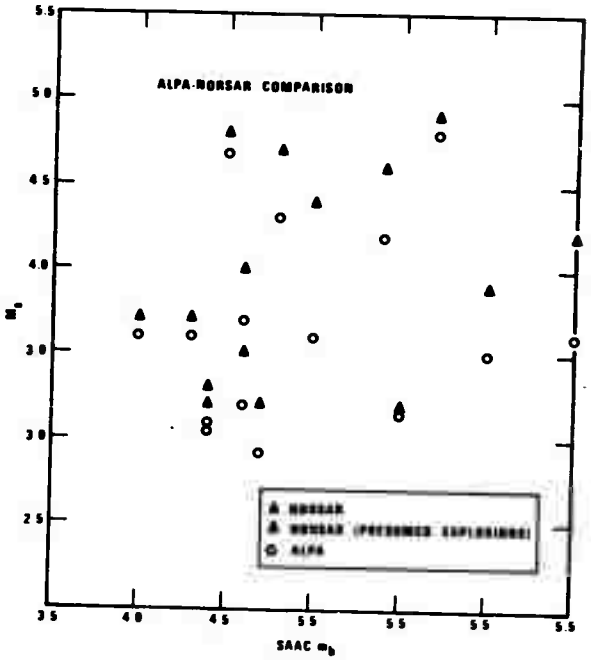

Figure 6. NORSAR M_s:m_b measurements for a set of events from central Asia and the western Soviet Union.

Figure 7. ALPA M_s:m_b measurements for a set of events from central Asia. The m_b values are the ones reported in the SAAC Daily Event Summary.

Figure 8. A comparison of M_s:m_b measurements for NORSAR and ALPA from a common set of central Asian events. The m_b values are the ones reported in the SAAC Daily Event Summary.

ALPA. When the two sets are directly compared, as shown in Figure 8, a significant result emerges. In all cases for earthquakes the M_s value calculated at NORSAR is higher than the same value at ALPA. The minimum separation is 0.2 M_s units and the maximum is 0.8 M_s units. Again, as in the LASA-NORSAR comparison, the travel paths are geologically different. The path to NORSAR traverses stable continental and shield structure whereas Rayleigh waves recorded at ALPA travel from a continental source skirt the Arctic Ocean basin and pass into the tectonically complex Alaskan region. Spatial coherence studies have shown that surface waves generated in central Asia exhibit very little variation across the NORSAR array, whereas there is quite a significant amount of variation across ALPA. During quiet periods the RMS background noise level is approximately the same for the two arrays for beams focused towards central Asia (Texas Instruments, Inc., personal communication). This implies that NORSAR is a better long period array than ALPA for detection of surface waves generated in the central Asian region. The few M_s values calculated at LASA for events in this area indicate that NORSAR again has systematically higher values.

In Figure 9 a composite set of M_s:m_b values is given for the central Asia-western Soviet Union region. All the earthquakes are recorded by ALPA or NORSAR. In cases

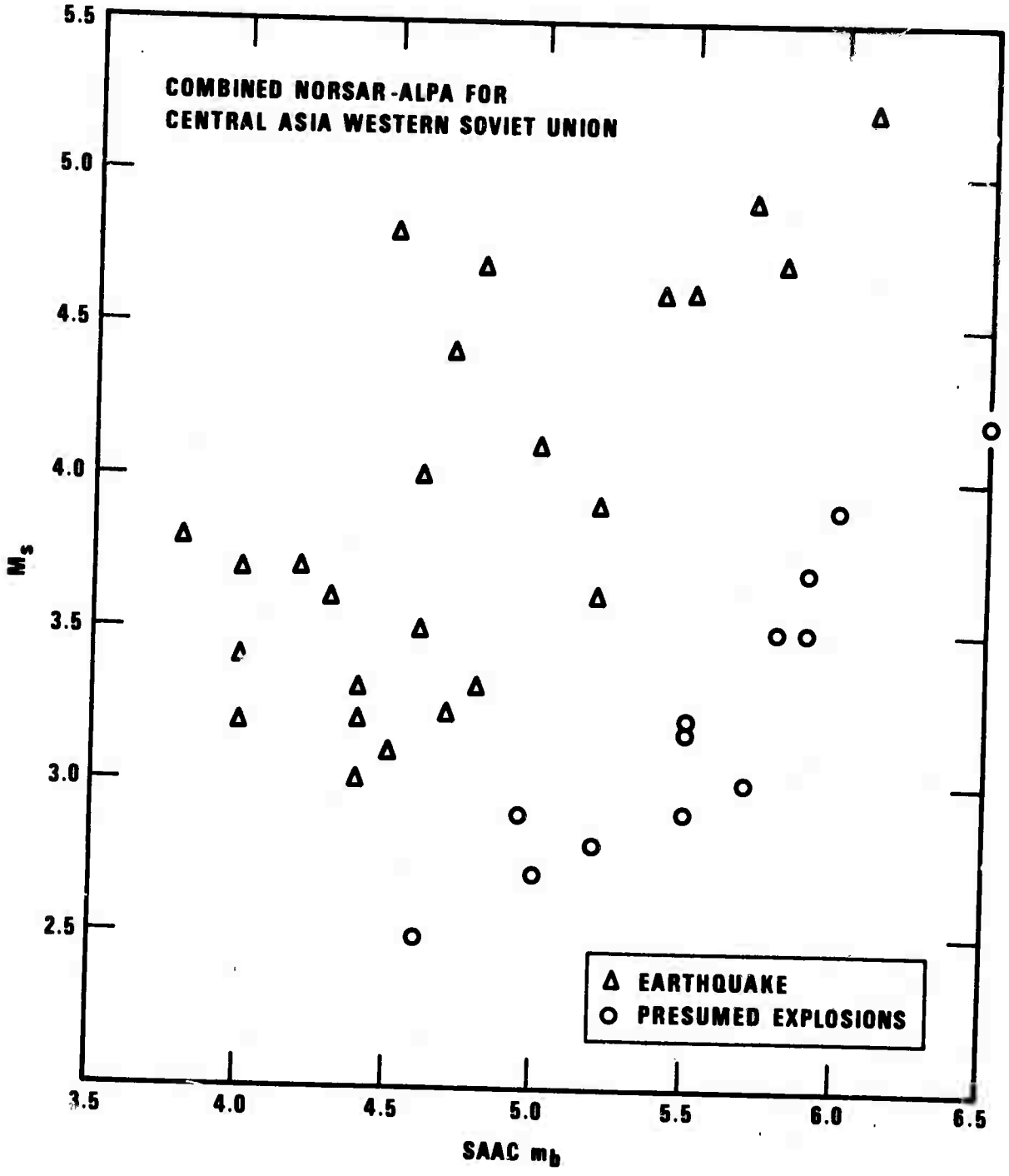

Figure 9. Combined NORSAR-ALPA M_S:m_b measurements for a set of events from central Asia and the western Soviet Union.

where both arrays recorded the event the higher M_s value (always NORSAR) is used. The same applies to the presumed explosions, the higher value being used also. A few values for presumed explosions recorded at LASA early in 1971 have been included. These are all documented in Appendix III. A good separation is maintained between earthquakes and presumed explosions.

The lack of small amplitude events would make it somewhat presumptious to talk in terms of a threshold of detection. However, using the frequency beamforming techniques described in Appendix I an M_s value as low as 2.5 has been measured at NORSAR for a western Soviet Union source and an $M_s = 2.6$ at ALPA, and for the central Asian region the lowest values so far measured are 2.7 and 2.9 for NORSAR and ALPA respectively.

Although NORSAR is appearing to be a very good LP array for events from the east, there is at least one potentially serious handicap. Coherent noise, at Rayleigh wave velocity, has been observed propagating from an azimuthal range 50° to 90°. In one particular case this noise interfered with the reception of a Rayleigh wave generated by a presumed explosion in the estern Soviet Union. This example was shown in SAAC Report No. 4. The event was detected at LASA and ALPA, a fact which establishes the value of the network, but, for smaller sources, NORSAR is the only array capable of making a detection, owing to its proximity to western USSR.

Conclusions

The current analysis indicates that NORSAR is the best of the three large arrays for detecting and measuring Rayleigh waves from central Asia and the western Soviet Union. This is not just due to the fact that it is closer but also because signals show virtually no degeneration across the array. However, the occurence of the coherent noise, observed at NORSAR propagating from the east, establishes that at least a second array, in this case ALPA, is necessary to avoid misidentification.

Analysis of small events is now in progress to estimate a network threshold but so far we know only that signals with M_s = 2.7 in central Asia and 2.5 in western Soviet Union have been identified.

The NORSAR-LASA study of Kuriles events shows that for $m_b \geq 4.0$ interference from events in adjacent seismic regions was the main cause of non-detection. In the data set used, which was derived from the LASA/SAAC Daily Event Summary, all events with $m_b \geq 4.0$ were detected when no interference was present, with a detection at just one array (and not necessarily the other) being considered a true detection. The wave amplitudes at NORSAR were generally larger than the equivalent amplitudes at LASA A simpler propagation path and better signal coherence at NORSAR is considered to explain this difference.

V. CURRENT AND FUTURE WORK

The current LP processing system can analyze the LP data from all three arrays, looking for and measuring Rayleigh waves associated with all events reported by the LASA and NORSAR event summaries, all at a real-time rate. However, this complete analysis requires an inordinate amount of 360/44 time, considering the general computer requirements of SAAC, and so feasibility tests are being done to see how much LP analysis can be performed on a routine basis using both the 360/44 and the 360/40B. Currently all events from the Sino-Soviet and adjacent regions reported by the LASA or NORSAR event summaries are routinely analyzed, and these data are being collected for presentation in a later report.

A comparison study between f-k analysis and a quasi-matched filtering scheme is being initiated. The filters are derived from composite group velocity curves generated for any source-receiver combination. This particular matched filtering approach is being used because it is considered to be the only one capable of handling many events routinely.

REFERENCES

Dean, W. C., et al., 1971, SAAC Technical Report No. 1, SAAC Evaluation of the SAAC/LASA system, Teledyne Geotech, Alexandria Laboratories (Aug. 1971), ARPA Order No. 1620

Lacoss, R. T., 1971, Magnitudes and source character, Semiannual Technical Summary, Lincoln Laboratory, M. I. T (30 June 1971) ESD-TR-71-191

Mack, H., 1971, SAAC Technical Report No. 4, Evaluation of the large array long-period network, Teledyne Geotech, Alexandria Laboratores (Dec. 1971), ARAP Order No. 1620

Mack, H. and E. A. Flinn, 1972, Spatial coherence of short period acoustic-gravity waves. Geophys. J. Roy. Astron. Soc., (in press)

Marshal, P. D. and P. W. Basham, 1972, Discrimination between earthquakes and underground explosions employing an improved M_s scale, Geophys. Journ. Roy. Astron. Soc., (in press)

Smart E., and E. A. Flinn, 1972, Fast frequency wave-number analysis and Fisher detection in real-time infrasonic data processing, Geophys. J. Roy. Astron. Scc., (in press)

ACKNOWLEDGEMENT

This research was supported by the Advanced Research Projects Agency, Nuclear Monitoring Research Office, under Project VELA-UNIFORM, and accomplished under the technical direction of the Air Force Technical Applications Center under Contract F33657-71-C-0510.

APPENDIX I.

Frequency-Wavenumber Analysis

It was mentioned in the text that frequency-wavenumber (f-k) analysis is nothing more than beamforming in the frequency domain. The method takes advantage of the fact that the signal-to-noise ratio is frequency dependent and so the beamforming is done frequency by frequency. Also by staying in the frequency domain a great many beams can be examined rapidly. In practice this means that the azimuth and velocity of a signal need not be assumed; one merely accepts the beam with the maximum power. The position of this maximum in the wavenumber domain defines the azimuth and velocity of the signal. The process is defined by the expression (Smart and Flinn, 1972):

$$P(f,\underline{k}) = N^{-2} \left| \sum_{n=1}^{N} A_n(f) \exp[2\pi i(\phi_n(f) - \underline{k} \cdot \underline{r}_n)] \right|^2 \qquad (1)$$

where $A_n(f)\exp[i\phi_n(f)]$ is the Fourier transform of the n'th channel located at position vector $\underline{r}_n$. This expression represents a three-dimensional space with frequency being one dimension and the wavevector $\underline{k}$ being the other two. For computation $\underline{k}$ is resolved into a Cartesian coordinate system with k_y related to geographic north for a particular array and k_x related to geographic east. For a particular time window this space is searched for maxima, the position of each maximum defining the

velocity and azimuth of wave motion propagating coherently across the array. The power of a maximum, $P(f,\underline{k})$, is the signal power estimate at frequency f, and the signal-to-noise ratio estimate is defined as:

$$S/N = \frac{P(f,\underline{k})}{A_v(f) - P(f,\underline{k})} \qquad (2)$$

where Av(f) is the average channel power at frequency f. Obviously this estimate is better for high signal-to-noise ratios. For a particular array geometry, expression (2) has a minimum value above which it is certain that a detection was not made via an array side-lobe. Below this particular minimum value a detection may or may not have been made by a side-lobe. Expression (2) is also indicative as to the goodness of the estimate of signal power P(f,k). The higher the S/N value the better the estimate.

An example of how effective a frequency domain beamforming technique can be is illustrated in Figure 10. The beam trace of a Rayleigh wave originating in the Kurile Islands and recorded at LASA was added to LASA noise, from the same beam. The amplitude of the signal was successively lowered but the noise was held at constant amplitude and at each step the data were subject to the described analysis. The top trace in Figure 10 shows the noise, with an RMS value of 6 mμ

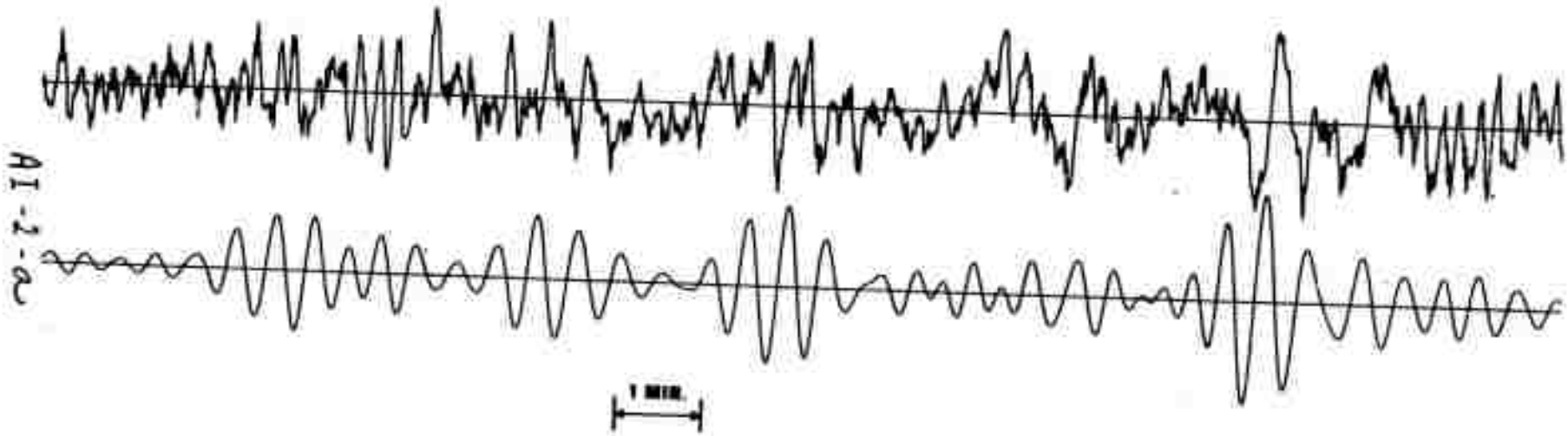

Figure 10. Unfiltered and filtered seismogram consisting of beamed LASA noise and added signal. f-k Analysis picked this signal and assigned the correct azimuth and velocity.

(relative to the 25 second period calibration). The signal, with a peak-to-peak value of 12 mμ, has been added but is quite invisible. This is now equivalent to an M_s value of 2.6 as recorded at LASA. The lower trace is the same data filtered with a bandwidth of 20 to 40 seconds period. The signal is now visible but is distorted by the additive noise and is indistinguishable from other wave groups which have been passed by the beam. However, the described method of f-k analysis assigned the correct azimuth and velocity to the signal and assigned other azimuths and velocities to the other wave groups. This experiment was repeated three times using different noise and in each case the results were essentially the same. One may argue that similar results might be obtained in the time domain by very narrow band filtering and forming a great number of closely spaced beams. This may be true, but the computation time involved would be very much longer.

As was mentioned in the main text, the interference of two separate Rayleigh waves within the area of the array is a sufficiently common phenomenon as to warrent serious consideration in any processing scheme. Furthermore, using the relatively short time windows in the f-k analysis, the background noise appears to consist mainly of discrete Rayleigh wave trains arriving from many azimuths. These wave trains interfere with small expected arrivals in much the same manner as two larger events.

If two Rayleigh waves are of comparative size, f-k analysis usually detects the presence of both, and assigns the appropriate azimuths and velocities as the time window moves through the event, because it is highly unusual for the two waves to exhibit identical time-frequency histories in the array region. However, signal power estimates may be in error even though the events were correctly identified. Also, if one event is really dominant then it may completely mask the smaller arrival For such cases a filtering scheme has been devised (Smart, personal communication) whereby the f-k space maxima are removed, along with associated side-lobes, allowing the detection of secondary maxima. This process, referred to as stripping, is accomplished by removing the signal estimate from each channel in the complex frequency domain, frequency by frequency. Specifically, the transform of the j'th channel after signal subtraction, $F'_j(f)$, is expressed as

$$F'_j(f) = \left[F_j(f)\exp[-2\pi i \underline{k}\cdot\underline{r}_j] - \frac{1}{N}\sum_{j=1}^{N} F_i(f)\exp[-2\pi i \underline{k}\cdot\underline{r}_j] \right]\exp[2\pi i \underline{k}\cdot\underline{r}_j]$$

An example of this stripping process was given in SAAC Report No. 4. In that particular case two signals were added as though recorded at ALPA from two distinct azimuths with a 20 db difference in signal size. It is much more satisfactory to illustrate the process with real situations, and two such examples are given in this report. The first example illustrates the separation of two unequal but azimuthally distinct signals recorded by ALPA. The wavenumber plane, for a period of 18.3 seconds, is shown in Figure 11. An arrival from an azimuth of 65^{o} is dominant and there is only a suggestion of a second signal 12 db down from an azimuth of 187^{o}. This same plane is shown in relief in Figure 12 which effectively illustrates the signal power difference. Figures 13 and 14 show the wavenumber plane and the relief version after application of the stripping process. The second signal is now quite clear and is in fact dominant.

The second example shows how a small signal was detected at ALPA in the presence of another small signal and noise. The wavenumber plane and relief version are shown in Figures 15 and 16 respectively. The signal of interest is masked by another one close by. After stripping, Figures 17 and 18 show the second smaller signal quite clearly. This small signal occurred at the expected arrival time at ALPA of a Rayleigh wave from a small presumed explosion (SAAC $m_b = 4.9$) in the

western Soviet Union. The signal amplitude is calculated as 11 mμ corresponding to a surface wave magnitude, M_s, of 2.6. For comparison the time domain beam plot is shown in Figure 19 and it is obvious that a pick could not be confidently made at the expected arrival time because the signal is indistinguishable from other disturbances.

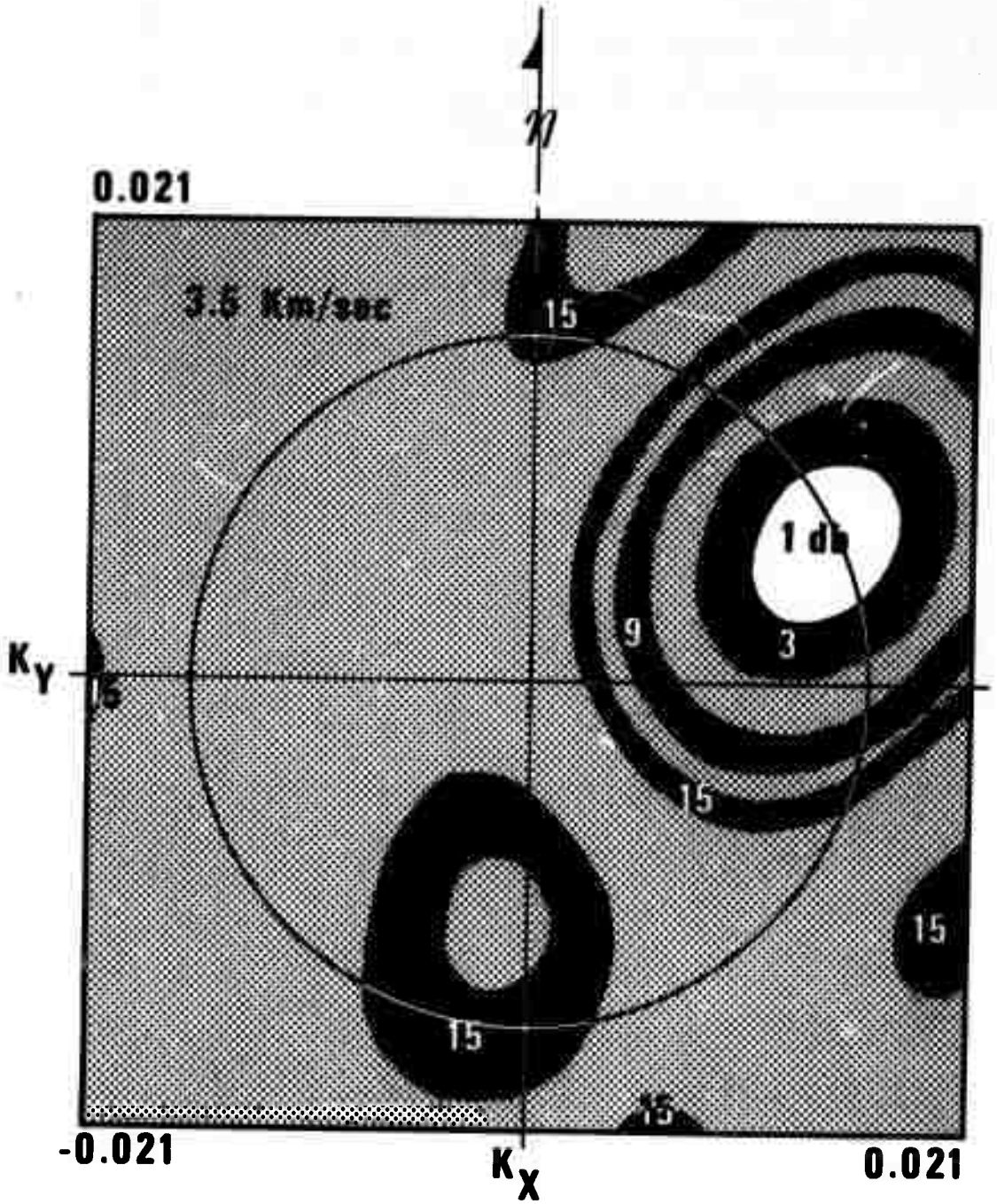

Figure 11. Wavenumber plane at a period of 18.3 sec for ALPA on 4 October 1971 for the time interval 1037 48.0 - 1042 3.0 GMT. The suspected smaller signal is 12 db down from the main dominant peak.

AI-6-a

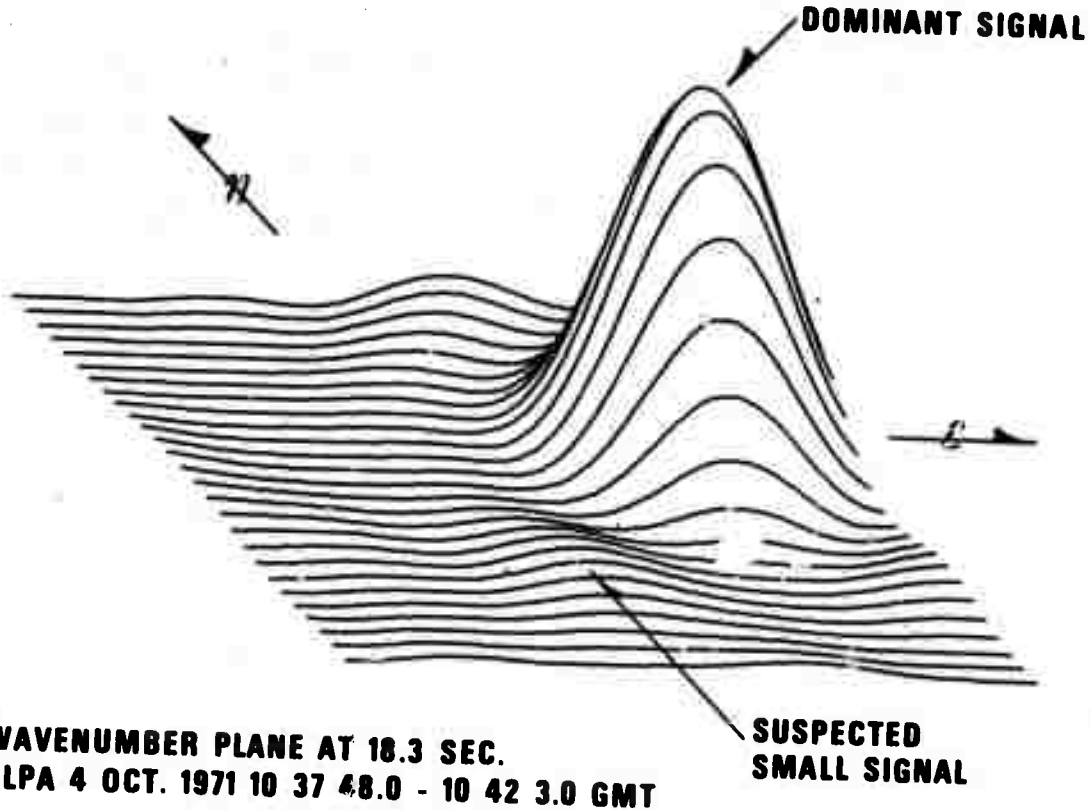

Figure 12. Relief illustration of the wavenumber plane shown in Figure 11.

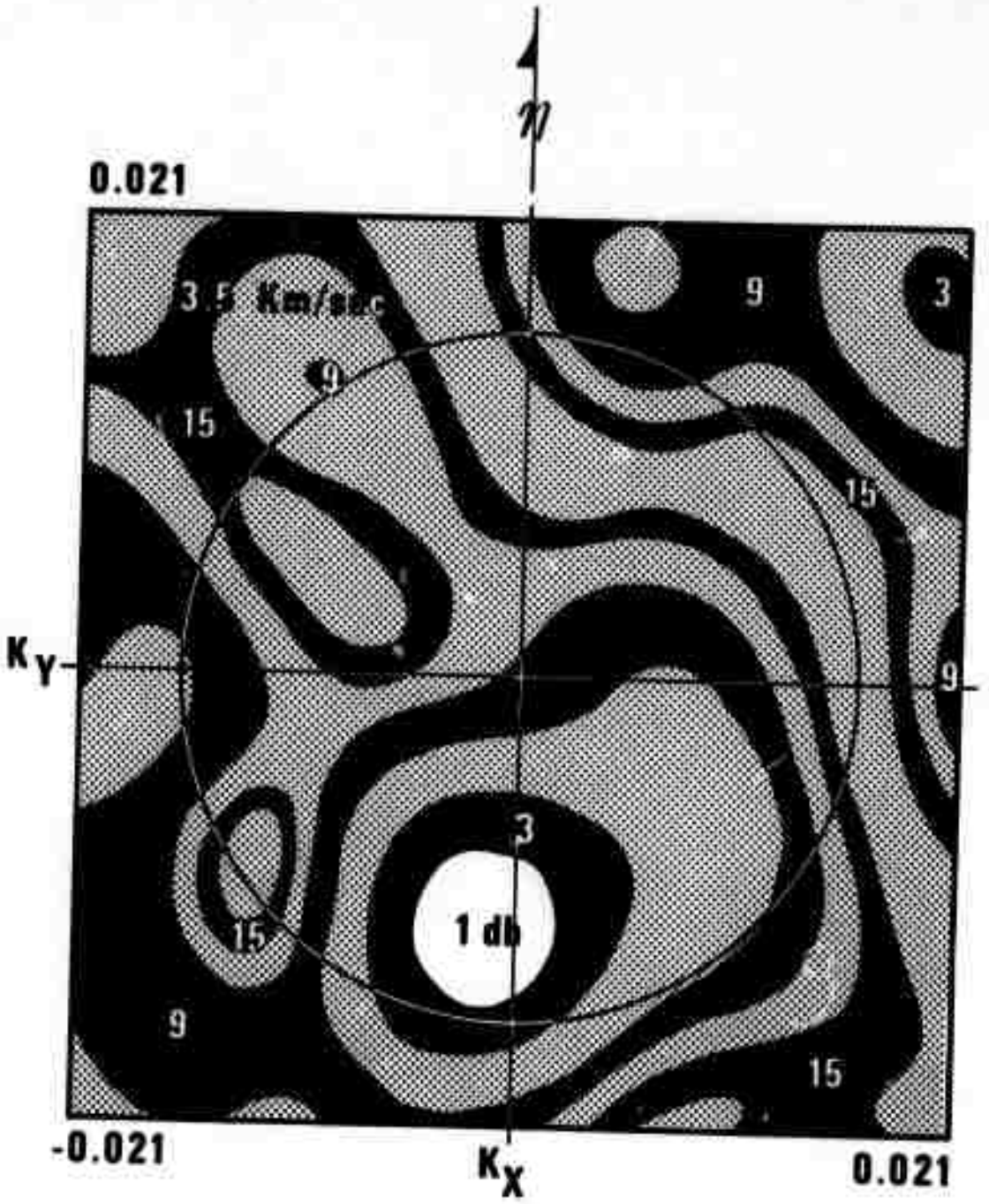

Figure 13. The wavenumber plane shown in Figure 12 after removal of the dominant signal by the stripping process.

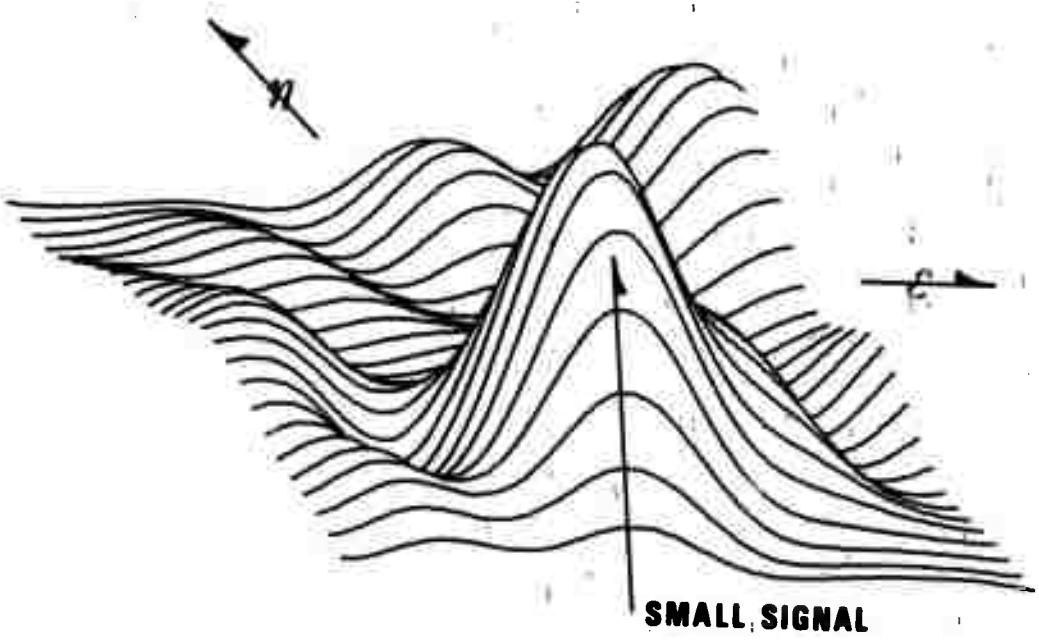

WAVENUMBER PLANE AT 18.3 SEC.
ALPA 4 OCT. 1971 10 37 48.0 - 10 42 3.0 GMT (After stripping)

Figure 14. Relief version of the wavenumber plane shown in Figure 13.

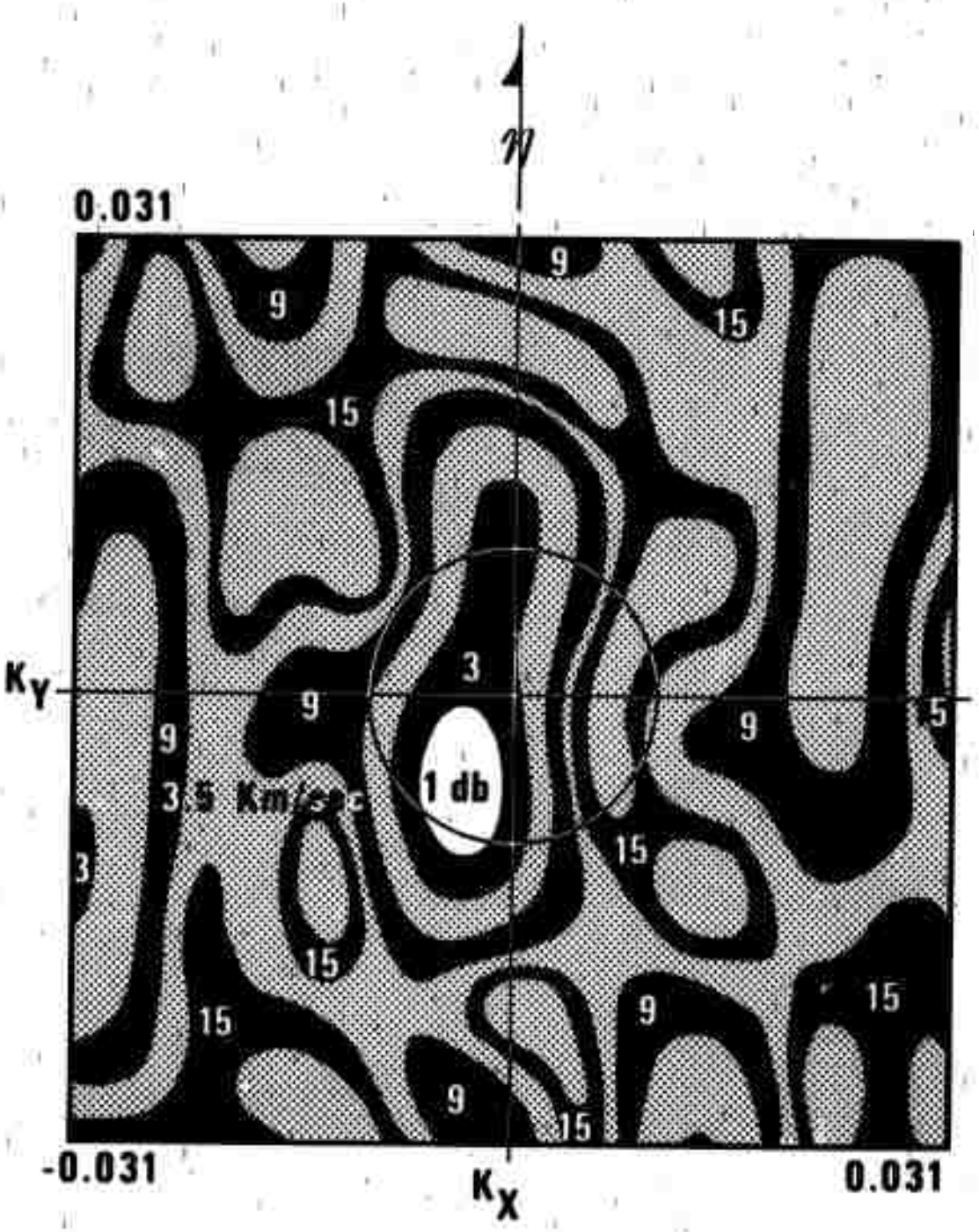

Figure 15. Wavenumber plane for ALPA on the 19 September 1971 for the time interval 1125 00. - 1129 15.0 GMT. The period is 26.9 sec. The smaller hidden arrival to the north is merged with a slightly larger arrival to the southwest.

AI-6-e

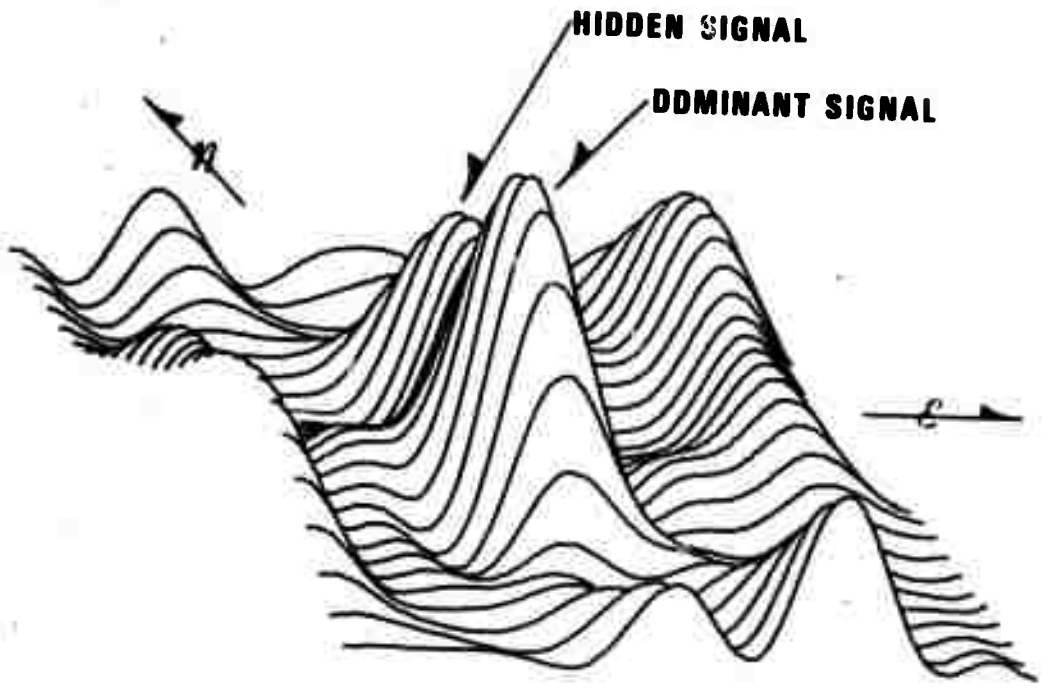

Figure 16. Relief version of the wavenumber plane in Figure 15.

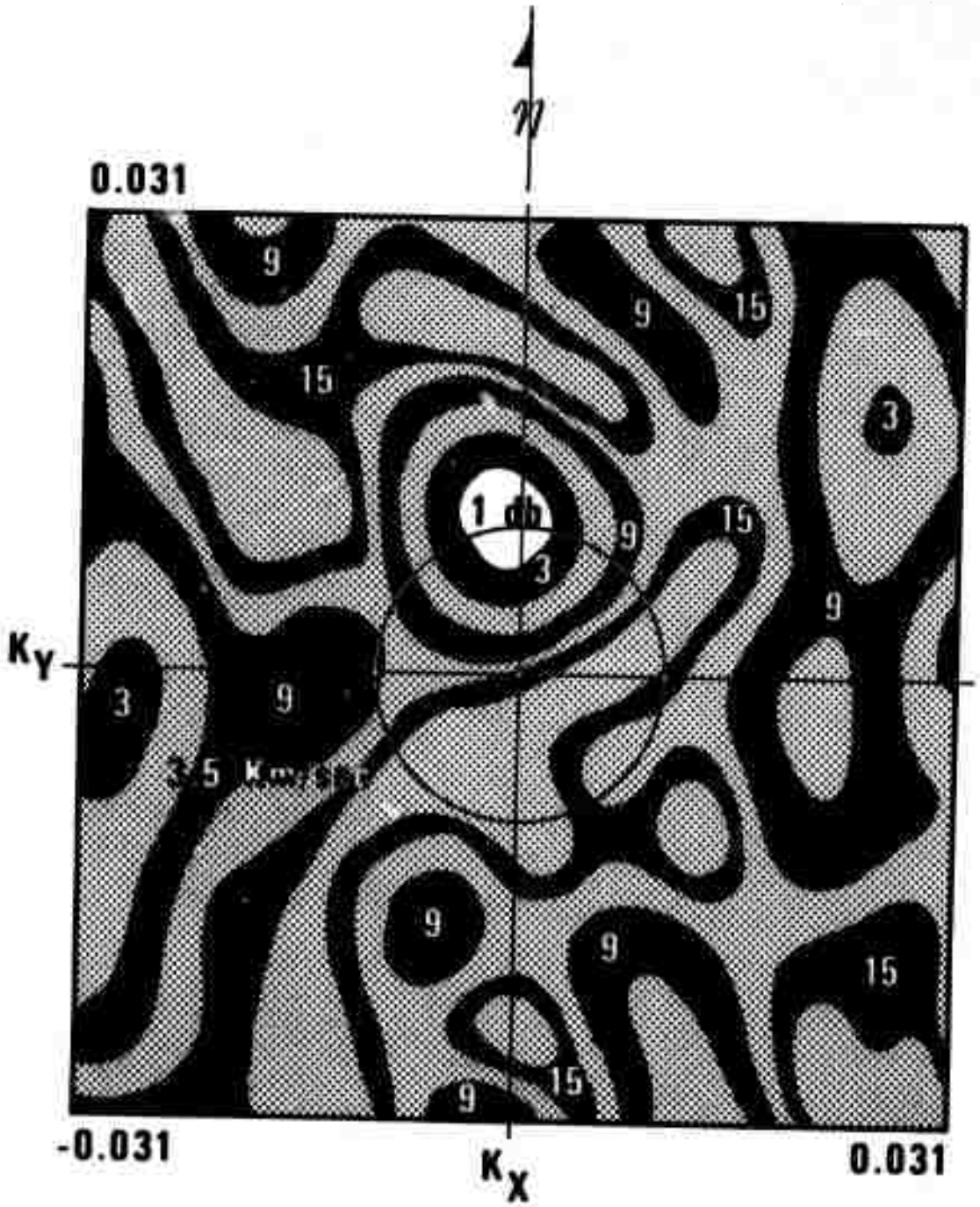

Figure 17. The same wavenumber plane as in Figure 15 after removal of the interfering signal by the stripping process. The second signal is now distinctly resolved.

AI - 6. g

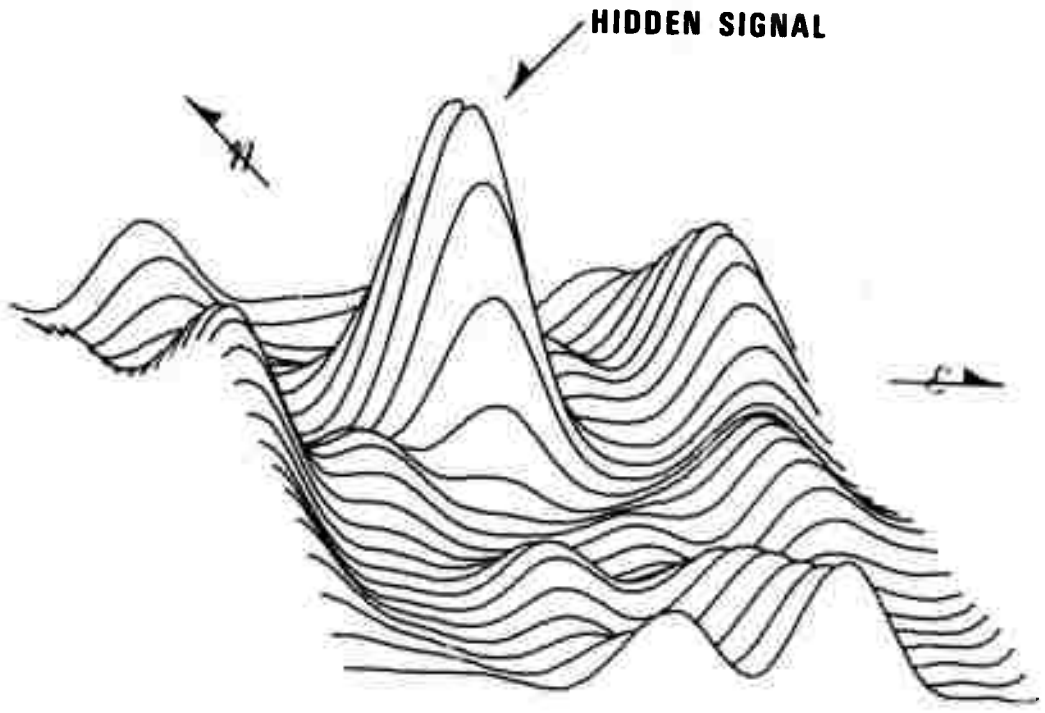

WAVENUMBER PLANE AT 26.9 SEC.
ALPA 19 SEPT. 1971 11 25 0.0 - 11 29 15.0 GMT (After stripping)

Figure 18. Relief version of the wavenumber plane shown in Figure 17.

AI-6-h

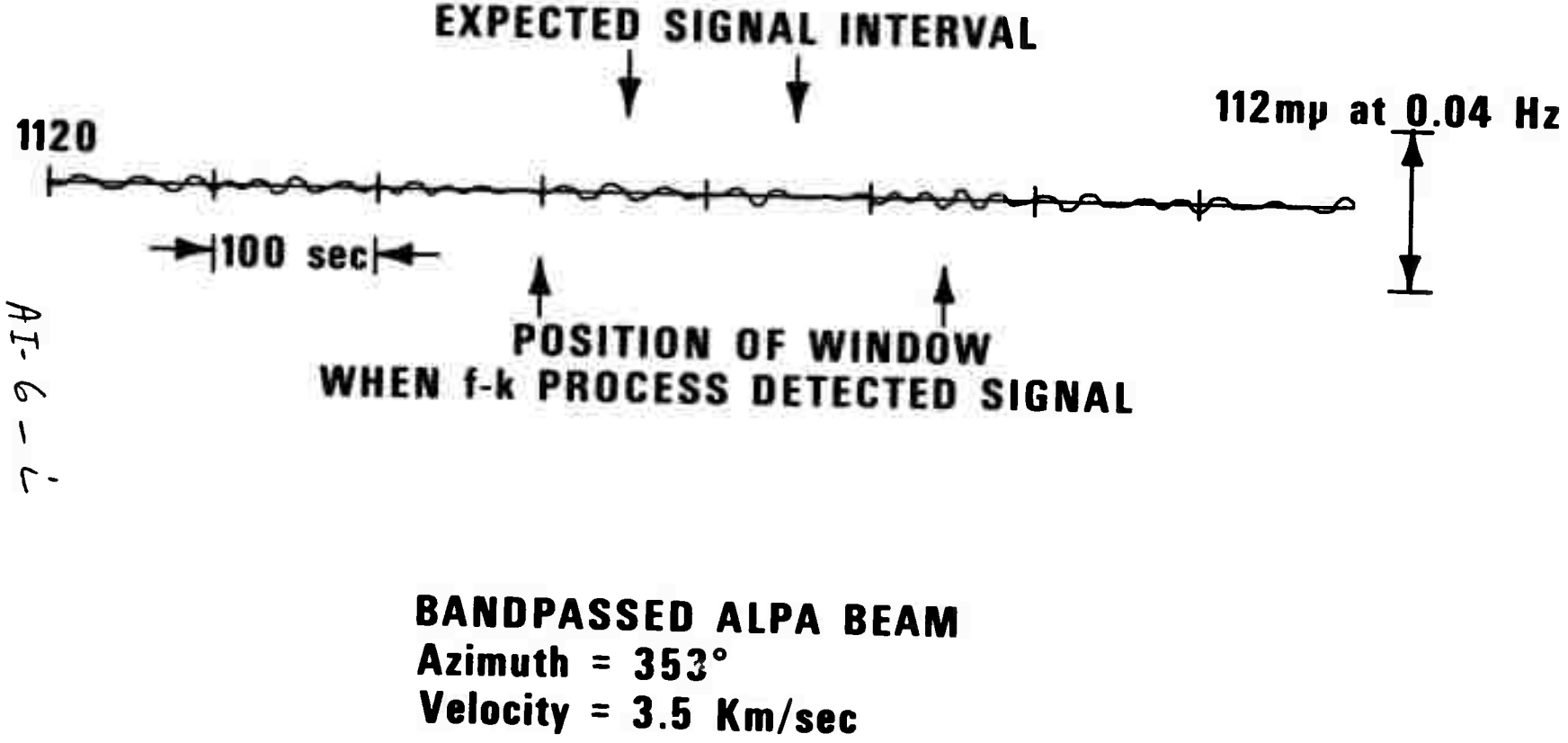

AI-6-1

Figure 19. Time-domain ALPA beam plot showing the window used in the f-k process. The ambiguity of single time domain plots is well illustrated.

APPENDIX II.

M_s Measurement

As was stated in the main text, one reason a frequency domain analysis scheme has been devised is because of the large volume of array data to be processed in real-time. However, for discrimination purposes the ground motion amplitude of the surface waves is desired in order to calculate the surface wave magnitude M_s. This is conventionally done by picking the maximum excursion on a time-domain plot. To avoid confusion the M_s values given in this report are what would be obtained by measuring amplitude from a beam plot and applying the formula

$$M_s = \log A/T + \log \Delta + 1.12$$

where the symbols have their usual meaning. The signal power estimate for a particular source region, array and time window length is empirically related to the ground motion amplitude of surface waves obtained from time-domain beams with good signal-to-noise ratios. To illustrate how this relation is obtained, a large amplitude Rayleigh wave from the Kurile Isles was added to beamed noise of NORSAR and LASA. A series of f-k analyses were run with successively reduced signal amplitudes, and the square root of the signal power estimate was plotted as a function of maximum signal amplitude. The results for

LASA are shown in Figure 20. A good linear relationship is obtained for higher amplitudes with a small deviation as the amplitude approaches zero resulting in a finite power associated with the noise. The slope of the line is the empirical relation between surface wave amplitude and the square root of the signal power estimated from the f-k analysis procedure. For any particular region this relationship is obtained as a function of distance from the array. To illustrate the reliability of the method Figure 21 shows the comparison between M_s values measured from beam plots and from the f-k power for a set of Kurile events recorded at NORSAR and LASA. The points are seen to cluster around a line of unit slope. The small amount of scatter is understandable. For one reason the period which has the dominant power according to the f-k analysis, very rarely agrees exactly with the period of the maximum amplitude measured from the seismogram. Another is that the signal power estimate varies slightly depending on the position of the window relative to the maximum amplitude on the seismogram. This effect decreases with increased overlap of time windows. However, the trade-off for this improvement is increased processing time for a given record length. Practically speaking, a 25% overlap is found to be sufficiently accurate for events further than 40^{o} from the array. For closer distances, western Soviet Union to NORSAR for example, a 50% overlap is used.

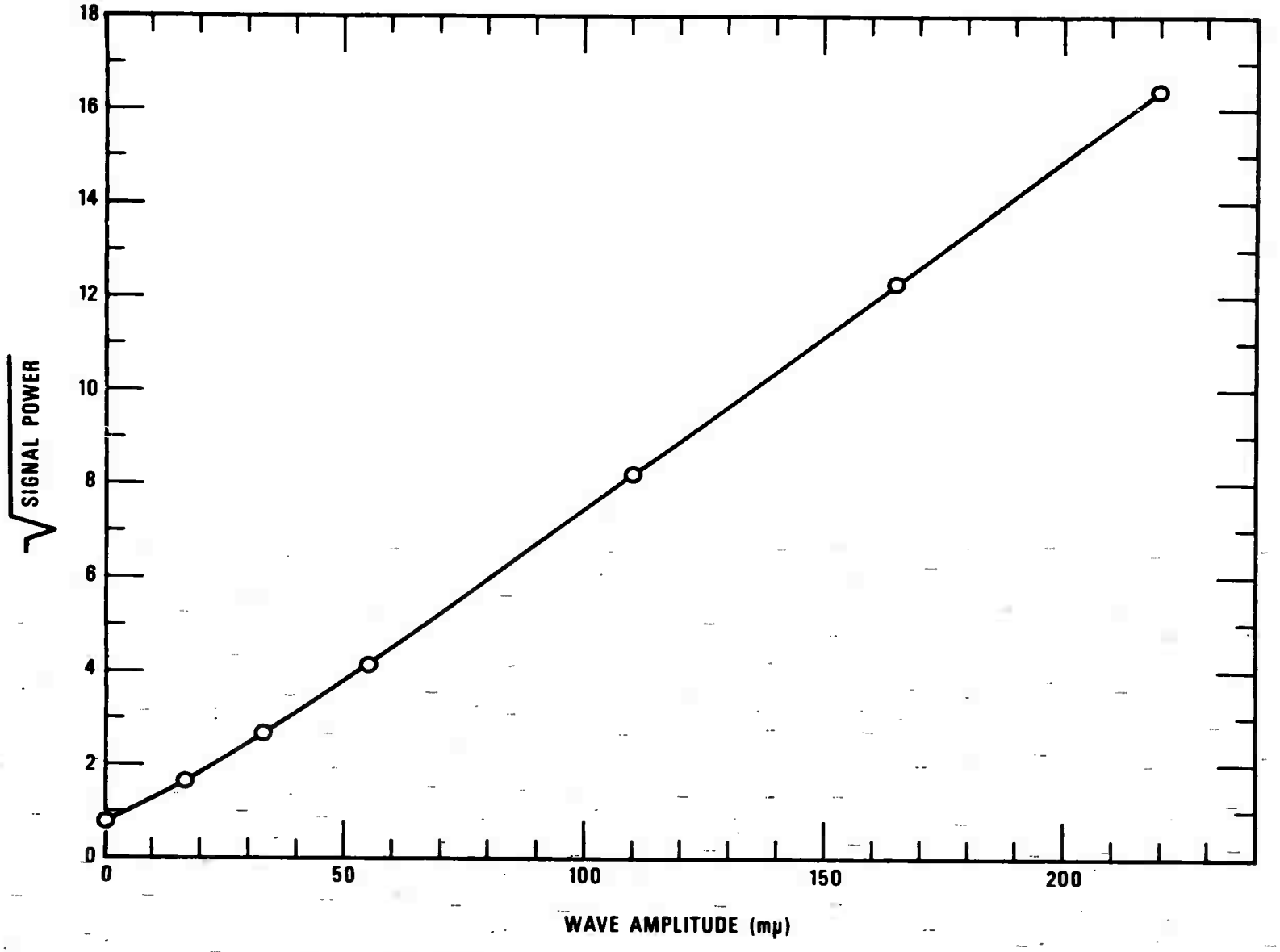

AII-2-4

Figure 20. Square root of the signal power estimate from f-k analysis versus maximum ground amplitude for a Rayleigh wave from the Kurile Islands region recorded at LASA.

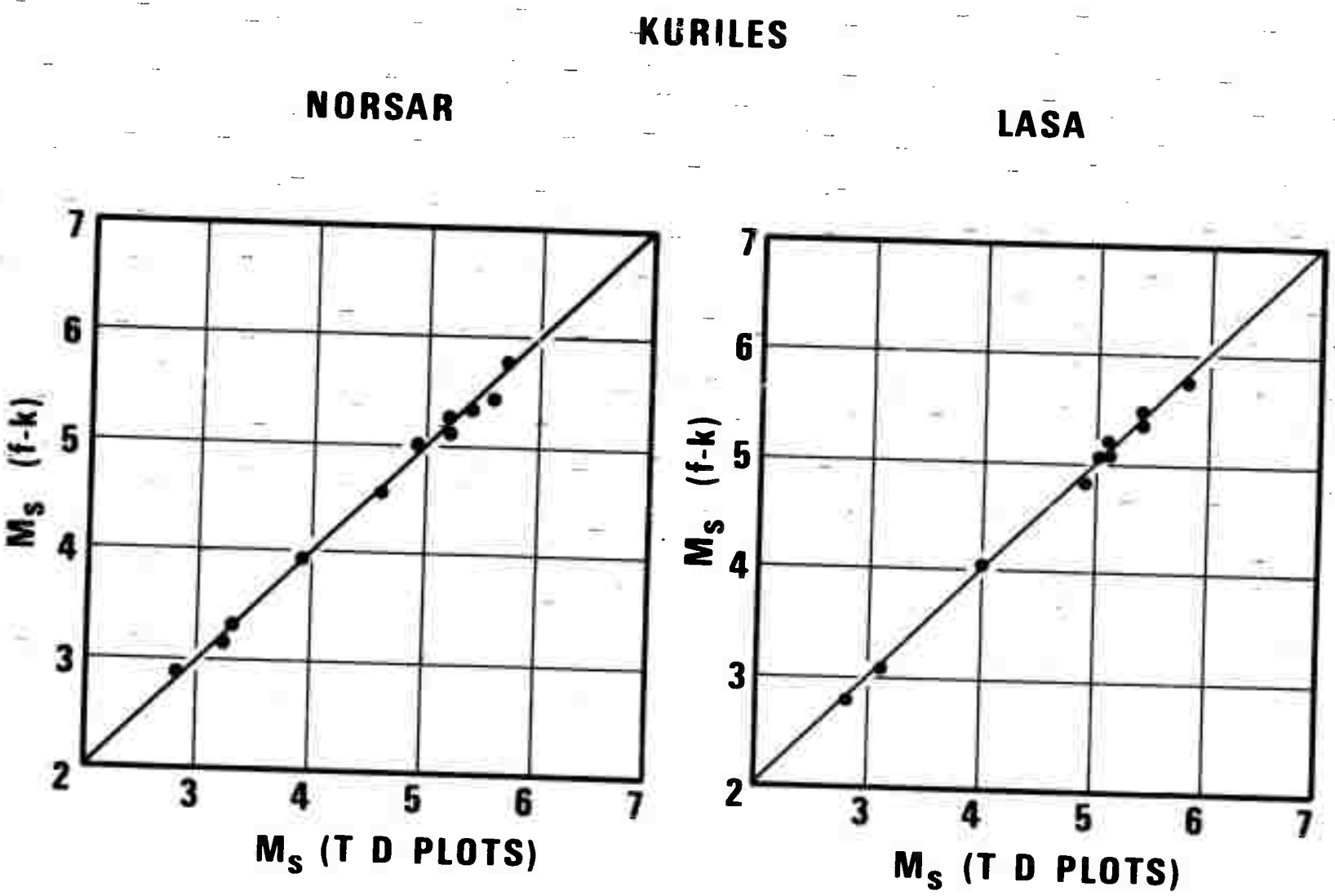

AE-2-C

Figure 21. A comparison of M_S values measured from f-k analysis and time domain beam plots for Rayleigh waves generated in the Kurile Islands region and recorded at NORSAR and LASA.

All in all, the conventional and f-k methods of measuring M_s agree very closely. The advantages of f-k are speed, automatic selection of the period with highest signal-to-noise ratio, and the certainty that the power measurement used is truly from the beam of interest.

APPENDIX III.

Table of events analyzed and used for this report. The body wave magnitude m_b is the value reported by the SAAC Daily Event Summary. Under each array name is the surface wave magnitude M_s if detected and measured. A star (*) signifies the Rayleigh wave was not detected and the letters BD indicate bad data on the low rate tape at the expected Rayleigh wave arrival time. If the LP data were not processed up to the time of this report a gap has been left. The letter I denotes that strong interference from an adjacent seismic region prevented any possible detection being made.

KURILE ISLANDS REGION

Date	Arrival Time (LA0)	Location	SAAC m_b	LASA M_s	NORSAR M_s	ALPA M_s
2 May 71	15 13 30.7	46N151E	4.2	3.0	3.0	
4 May 71	18 10 35.9	50N156E	4.2	3.3	3.8	
6 May 71	9 02 56.8	49N156E	4.0	3.0	3.0	
12 May 71	21 51 20.9	48N154E	4.8	3.6	3.7	
15 May 71	21 14 49.3	43N148E	4.1	3.6	4.1	
22 May 71	7 43 25.2	44N147E	4.1	3.3	3.4	
26 May 71	1 57 15.9	44N147E	4.5	3.8	3.9	
29 May 71	0 26 27.9	45N149E	5.5	3.9	3.9	
30 May 71	0 32 21.9	46N151E	4.5	3.4	3.4	
31 May 71	3 49 37.7	49N156E	4.0	I	I	
5 Jun 71	6 6 59.4	44N147E	4.2	2.7	2.9	
12 Jun 71	22 36 44.9	45N148E	5.3	3.9	BD	
16 Jun 71	9 15 48.3	48N154E	4.1	3.2	BD	
17 Jun 71	9 43 1.7	45N149E	5.0	3.2	BD	
27 Jun 71	6 0 36.4	44N148E	4.0	2.8	BD	
27 Jun 71	20 16 43.3	46N151E	4.1	3.2	BD	
30 Jun 71	11 30 3.8	45N148E	4.5	2.9	BD	
3 Jul 71	16 28 11.9	49N156E	4.0	3.2	3.1	
9 Jul 71	6 50 49.1	44N148E	4.9	I	I	

Date	Arrival Time (LA0)	Location	SAAC m_b	LASA M_s	NORSAR M_s	ALPA M_s
9 Jul 71	8 17 36.6	43N148E	4.8	I	I	
9 Jul 71	16 55 18.6	43N148E	4.5	4.4	4.9	
9 Jul 71	17 22 59.5	43N148E	4.1	3.6	4.3	
9 Jul 71	18 5 54.8	43N148E	4.1	3.9	4.2	
10 Jul 71	9 12 22.9	45N151E	4.3	3.2	3.2	
10 Jul 71	14 39 56.8	44N149E	4.3	3.5	3.6	
12 Jul 71	6 19 18.3	45N149E	4.6	BD	3.2	
12 Jul 71	20 2 9.8	46N151E	4.5	BD	BD	
18 Jul 71	12 42 37.6	51N157E	4.3	*	2.9	
22 Jul 71	23 7 20.8	44N149E	4.3	3.5	BD	
25 Jul 71	0 51 38	50N154E	4.1	3.1	2.9	
25 Jul 71	8 46 20.4	44N147E	4.0	3.3	2.9	
25 Jul 71	16 49 57.8	45N151E	4.6	I	I	
27 Jul 71	20 13 25.6	46N149E	4.1	I	I	
28 Jul 71	2 50 26.8	46N155E	4.1	I	I	
30 Jul 71	10 44 2.2	49N156E	5.0	3.8	3.8	
1 Aug 71	2 16 12.6	51N158E	5.7	4.9	5.0	
1 Aug 71	19 6 6.9	44N149E	4.3	3.3	3.8	
3 Aug 71	10 21 14.9	49N154E	4.1	3.1	BD	

Date	Arrival Time (LA0)	Location	SAAC m_b	LASA M_s	NORSAR MM_s	ALPA M_s
5 Aug 71	11 6 31.9	45N151E	4.3	3.5	3.9	
11 Aug 71	19 14 5.4	44N153E	4.2	I	3.9	
12 Aug 71	8 24 58.1	46N151E	4.2	*	BD	
13 Aug 71	0 44 51.3	49N156E	3.7	*	2.9	
13 Aug 71	6 26 40.2	46N151E	4.1	2.9	3.0	
18 Aug 71	20 9 21.7	44N148E	4.6	3.6	4.0	
19 Aug71	22 25 51.4	49N155E	6.2	6.0	6.2	
23 Aug 71	22 6 1.9	46N156E	5.8	5.8	5.9	
24 Aug 71	10 3 35.9	46N151E	4.3	3.8	3.5	
26 Aug 71	3 23 59.8	45N153E	3.8	*	2.9	
30 Aug 71	15 17 43.6	44N148E	4.2	BD	BD	
1 Sep 71	11 4 22	48N155E	5.1	3.7	4.2	
4 Sep 71	15 20 57.3	45N151E	4.5	4.5	4.1	
5 Sep 71	16 32 26.7	43N147E	3.9	3.2	3.2	
9 Sep 71	10 36 10.2	46N150E	5.2	3.9	4.4	
9 Sep 71	23 11 59.9	45N150E	5.9	5.9	5.7	
11 Sep 71	11 46 32.7	45N152E	3.8	2.9	3.2	
15 Sep 71	0 46 17.1	48N152E	4.0	3.2	3.1	
19 Sep 71	22 57 58.5	45N152E	4.0	3.7	3.6	

Date	Arrival Time (LAO)	Location	SAAC m_b	LASA M_s	NORSAR M_s	ALPA M_s
22 Sep 71	20 38 37.6	44N148E	4.7	3.1	3.4	
25 Sep 71	9 13 23.0	45N149E	4.0	3.1	BD	
25 Sep 71	12 41 7.2	47N153E	4.1	3.1	2.9	
26 Sep 71	0 15 24.9	49N152E	4.3	3.0	3.0	
27 Sep 71	15 47 36.2	49N156E	5.7	BD	4.0	
11 Oct 71	1 40 19.4	46N150E	5.3	4.3	4.4	
11 Oct 71	20 12 45.1	50N153E	3.9			*
15 Oct 71	15 27 54.6	45N149E	3.9			*
19 Oct 71	12 36 47.8	47N155E	4.2	3.1	3.0	I
21 Oct 71	20 34 38.8	45N146E	4.0	2.9	2.9	BD
22 Oct 71	10 57 19.2	51N157E	3.8			*
24 Oct 71	17 16 43.8	48N156E	3.8	I	I	2.9
25 Oct 71	10 52 10.3	44N148E	3.9	2.8	BD	BD
27 Oct 71	8 35 49.3	48N152E	3.8	*	*	*
28 Oct 71	7 40 39.7	48N153E	4.7		3.5	BD
29 Oct 71	7 18 41.6	45N147E	4.0	3.1	3.3	BD
29 Oct 71	14 16 33.1	50N155E	5.9			4.5
29 Oct 71	19 55 38.3	50N152E	4.1	I	I	BD
30 Oct 71	9 38 2.9	50N154E	4.3	3.1	2.7	*

Date	Arrival Time (LA0)	Location	SAAC m_b	LASA M_s	NORSAR M_s	ALPA M_s
2 Nov 71	6 22 19.8	47N153E	4.1	*	3.1	2.8
3 Nov 71	8 53 44.6	49N149E	3.4	*	*	*
3 Nov 71	10 43 4.7	49N147E	4.8	3.6	3.9	3.3
4 Nov 71	8 0 32.4	50N155E	3.7		*	*
8 Nov 71	1 34 22.5	50N155E	3.9	3.2	I	*
9 Nov 71	2 46 48.5	44N148E	3.8		3.4	2.7
9 Nov 71	20 13 9.1	51N158E	4.3	3.0	3.2	I
13 Nov 71	4 15 20	44N147E	3.9		BD	2.6
13 Nov 71	7 36 32.2	44N147E	3.9		*	BD
18 Nov 71	6 51 0.4	49N154E	4.4	3.1	3.1	I
21 Nov 71	20 40 20.6	47N152E	4.1	3.1	*	*
23 Nov 71	8 38 32.1	44N155E	4.1		3.4	3.0
24 Nov 71	1 8 38	47N152E	5.4			3.9
28 Nov 71	17 58 16.2	49N155E	5.4			3.5
2 Dec 71	5 50 57.4	49N158E	4.7	3.3	2.9	BD
2 Dec 71	9 59 3.7	48N152E	5.0	3.4	I	3.1
2 Dec 71	17 29 2.8	43N150E	6.3	6.0	6.4	
3 Dec 71	6 22 43.4	44N154E	3.7			BD
3 Dec 71	19 23 38.4	48N153E	4.6		3.3	3.0

Date	Arrival Time (LA0)	Location	SAAC m_b	LASA M_s	NORSAR M_s	ALPA M_s
3 Dec 71	20 34 56.2	46N153E	4.1			2.7
4 Dec 71	16 12 9.2	45N147E	4.5		3.6	I
8 Dec 71	04 37 46.5	45N149E	4.0			2.7
8 Dec 71	22 04 44.6	45N150E	3.8			*
11 Dec 71	18 34 15.5	51N158E	3.8			2.5
		CENTRAL ASIA-WESTERN SOVIET UNION				
		NORSAR m_b values are given in parentheses				
4 Aug 71	0 37 47	35N 70E	5.7(6.0)		4.9	4.8
16 Aug 71	22 51 18	39N108E	4.3(5.2)		BD	3.6
24 Aug 71	16 45 32	50N100E	4.5		4.8	4.7
25 Aug 71	06 28 34	41N 77E	4.4		3.2	3.1
26 Aug 71	11 48 54	47N 75E	4.2		I	
8 Sep 71	22 48 07	42N 44E	4.7		4.4	
14 Sep 71	20 25 47	44N 45E	4.5		BD	I
19 Sep 71	06 57 33	43N 47E	4.4		3.0	*
30 Sep 71	11 01 42	45N 81E	4.0		3.7	3.6
30 Sep 71	12 55 57	49N 98E	4.3		3.7	3.6
2 Oct 71	11 04 18	40N 44E	3.8		3.8	BD
6 Oct 71	23 56 48	36N 71E	5.2(4.7)			3.6
8 Oct 71	09 33 27	41N 79E	4.4	3.2	3.3	3.1

Date	Arrival Time (LA0)	Location	SAAC m_b	LASA M_s	NORSAR M_s	ALPA M_s
10 Oct 71	09 18 47	43N 44E	4.0		3.4	
15 Oct 71	17 21 02	41N 48E	5.2(4.7)		3.9	
21 Oct 71	23 19 49	51N103E	4.8(4.4)		BD	3.3
28 Oct 71	13 44 05	38N 72E	5.8(5.3)		BD	4.7
28 Oct 71	14 22 40	37N 72E	4.6(3.9)		3.5	3.2
29 Oct 71	17 31 30	38N 89E	4.6(4.5)		4.0	3.7
1 Nov 71	05 42 50	46N 88E	4.8(4.9)	4.5	4.7	4.3
13 Nov 71	20 31 02	50N 40E	4.0		3.2	
14 Nov 71	01 13 08	38N 72E	5.0(4.7)	4.3	4.1	3.6
2 Jan 72	10 40 40	43N 87E	5.4(5.1)	I	4.6	4.2
5 Jan 72	12 16 17	38N 73E	4.5	*	3.1	*
6 Jan 72	06 43 48	39N 73E	4.7(4.8)	3.6	3.2	2.9
12 Jan 72	18 50 41	39N 75E	5.5	4.5	4.6	BD
14 Jan 72	02 16 25	38N 72E	4.6		*	*
		Presumed Explosions				
22 Mar 71	04 45 31	50N 78E	5.9	3.5	BD	BD
23 Mar 71	07 11 23	62N 56E	5.9	3.9	BD	BD
25 Apr 71	03 45 31	50N 78E	5.9	3.5	BD	BD
25 May 71	04 15 31	50N 78E	5.0		2.7	BD

Date Date	Arrival Time (LA0)	Location	SAAC m_b	LASA M_s	NORSAR M_s	ALPA M_s
10 Jul 71	17 11 06	65N 54E	5.3	3.0	I	BD
19 Sep 71	11 11 32	59N 38E	4.9	2.9	2.9	2.6
4 Oct 71	10 11 15	64N 44E	4.6		2.5	*
9 Oct 71	06 15 30	50N 77E	5.2	3.0	2.8	BD
21 Oct 71	06 15 30	50N 77E	5.5	3.2	3.2	3.2
22 Oct 71	05 12 17	52N 55E	5.7	2.9	BD	3.0
29 Nov 71	06 15 31	50N 78E	5.5	3.1	BD	2.9
15 Dec 71	08 05 31	50N 78E	4.6	*	*	*
22 Dec 71	07 12 27	48N 48E	6.5	4.0	4.2	3.6
30 Dec 71	06 33 31	50N 77E	6.0	3.4	3.9	3.5